C. R. Mecanique 346 (2018) 524–531

Contents lists available at ScienceDirect

Comptes Rendus Mecanique

www.sciencedirect.com

Model reduction, data-based and advanced discretization in computational mechanics

A door to model reduction in high-dimensional parameter space

Vers des modèles réduits dans les espaces de très grande dimension

Charles Paillet *, David Néron, Pierre Ladevèze

LMT (ENS Paris-Saclay, CNRS, Université Paris-Saclay), 61, avenue du Président-Wilson, 94235 Cachan cedex, France

ARTICLE INFO

Article history:
Received 12 December 2017
Accepted after revision 2 April 2018
Available online 2 May 2018

Keywords:
Reduced Order Model (ROM)
PGD
Multiparametric

Mots-clés :
Réduction de modèles
PGD
Multiparamétrique

ABSTRACT

Model reduction techniques such as Proper Generalized Decomposition (PGD) are decision-making tools that are about to revolutionize many domains. Unfortunately, their computation is still problematic for problems involving many parameters, for which one has to face the "curse of dimensionality". An answer to this challenge is given in solid mechanics by the so-called "parameter-multiscale PGD", which is based on Saint-Venant's principle. In this article, a model problem composed of up to a thousand parameters is presented, showing that the method is able to overcome the "curse of dimensionality".

RÉSUMÉ

Les modèles réduits, en particulier ceux basés sur la *Proper Generalized Decomposition* (PGD) sont des outils de conception qui s'apprêtent à révolutionner la simulation numérique. Malheureusement, pour les problèmes à grand nombre de paramètres, la « malédiction de la dimensionnalité » semble être une limitation majeure. Nous proposons, avec la *parameter-multiscale PGD*, une solution à ce problème basée sur le principe de Saint-Venant. Un cas test comprenant jusqu'à mille paramètres est présenté dans cet article et prouve que la méthode permet bien de s'affranchir de la « malédiction de la dimensionnalité ».

1. Introduction

Numerical simulation has made a forceful entry into design and analysis offices. This revolution, which is anything but complete, has entered a new stage, called simulation-driven "robust" design, and leads to a major scientific challenge: simulations should be performed in quasi real time. The key is a new generation of reduced-order methods that comprises essentially the Proper Orthogonal Decomposition (POD), the Proper Generalized Decomposition (PGD), and the Reduced-Basis Method (RB), the basics and recent developments of which are given in [1]. Problems that must be solved may involve

* Corresponding author.
E-mail addresses: paillet@lmt.ens-cachan.fr (C. Paillet), neron@lmt.ens-cachan.fr (D. Néron), ladeveze@lmt.ens-cachan.fr (P. Ladevèze).

https://doi.org/10.1016/j.crme.2018.04.009
1631-0721/

a very high number of degrees of freedom, with multiple scales or interactions between several physics and can be associated with variable or uncertain parameters. Model reduction methods, together with the notions of offline and online calculations, also open the way to new approaches where simulation and analysis of structures can be carried out almost in real time.

This work is based on the PGD, which was introduced in [2,3] for the treatment of nonlinear time-dependent problems in solid mechanics. Many developments have been made over the last thirty years: multiscale, multiphysics, stochastic or non-stochastic parameters, acoustics, large displacements and deformations... In [4], the interested reader can find a synthesis of most of the developments carried out in Cachan, where the LATIN method plays a central role. A number of tools are now mature and have been applied to industrial cases and then, are competitors of classical computational methods (see book [5]). The PGD not only makes it possible to construct reduced models that can be used in real time, but it also reduces drastically the whole calculation time in many situations. However, a major limitation is still the number of parameters that can be involved (no more than a dozen, as it will be discussed in the following). This paper starts with a brief description of the classical PGD, highlighting its limitations for problems of high dimension.

Several attempts have been made to solve problems with a large number of parameters. For example, enhancements can be introduced by iterative solvers with conditioner [6] or more complex approximations of the data structure. The PGD uses the so-called separated variable representation, or canonical decomposition, but other compressed high dimensional field descriptions has been introduced: Tucker tensors, Tensor Train format or Hierarchical Tucker format [7–11]. However, the generic formulation of those tools can be a limitation for our applications.

On the contrary, we develop in this paper a physically based approximation introduced in [12,13]. Our proposal, named "parameter-multiscale" PGD is built on the Saint-Venant Principle, which works for many models in Physics. This "principle" highlights two different levels of parametric influence, which drives us to introduce a multiscale description of the parameters and to separate a "macro" and a "micro" scale, as it is classically done for space or time [14]. To implement this vision, a completely discontinuous spatial approximation is needed. Thus, we use the Weak-Trefftz Discontinuous Method introduced in [15] and applied in [16] for the calculation of "medium frequency" phenomena. In this paper, we first recall the basics of the parameter-multiscale PGD. Then, new developments are introduced, the main one being the computation of the algorithm on a 3D problem up to the second iteration, which leads to very small errors. This is done for problems with more than a thousand parameters, which shows that the method is able to overcome the "curse of dimensionality". Additional results put forward the capability and the limits of the parameter-multiscale PGD for solving problems with numerous parameters.

2. Model problem

One considers an elastic media that occupies the domain $\Omega \subset \mathbb{R}^3$ divided into N subdomains or elements $\Omega_E, E \in \mathbf{E}$. The parameter μ_E is associated with the rigidity of Ω_E and, for the sake of simplicity, we consider that μ_E is a scalar belonging to $[-1/2; 1/2]$. Let us introduce $\underline{\mu} \equiv \{\mu_E\}_{E\in\mathbf{E}}$, the corresponding space being $\mathbf{\Sigma}_\mu$. Note that, for an isentropic material, the maximum number of independent parameters per subdomain or element is 2. After discretization, any spatial field is approximated by N degrees of freedom, and the problem to solve can be written as:

$$\begin{aligned} &\text{Find } \underline{X}(\underline{\mu}) \in \boldsymbol{X} \text{ where } \boldsymbol{X} : \left\{ \begin{array}{rcl} \mathbf{\Sigma}_\mu & \rightarrow & \boldsymbol{U} = \mathbb{R}^N \\ \underline{\mu} & \rightarrow & \underline{X}(\underline{\mu}) \end{array} \right. \text{ such that:} \\ &\forall \underline{\mu} \in \mathbf{\Sigma}_\mu \qquad \boldsymbol{A}(\underline{\mu})\underline{X}(\underline{\mu}) = \underline{F_d}(\underline{\mu}) \end{aligned} \tag{1}$$

where $\boldsymbol{A}$ is a linear positive definite operator depending on $\underline{\mu}$. $\underline{F_d}$ is a given loading that could also depend on $\underline{\mu}$, but which will be considered constant for the sake of simplicity.

Fig. 1 shows an illustration of the model problem. This is a cube submitted to a uniaxial traction displacement, the opposite face sliding freely along a fixed surface. The parameters $\underline{\mu}$ are proportional to the local Young modulus and could be interpreted as damage intensity.

3. The standard PGD

The standard parameter PGD is described in [17]. For practical details, the reader can refer to [1]. In this method, the "curse of dimensionality" is bypassed using a separated variable representation (2):

$$\underline{X}(\underline{\mu}) = \underline{X}(\mu_1, \ldots, \mu_N) \approx \underline{X}^M(\mu_1, \ldots, \mu_N) = \sum_{j=1}^{M} \underline{\widetilde{X}}^j \prod_{E\in\mathbf{E}} g_E^j(\mu_E) \tag{2}$$

where M is the number of modes of the approximation, $\underline{\widetilde{X}}^j$ a spatial vector and the g_E^j are functions of only one parameter μ_E.

At each iteration, a greedy procedure enriches the solution with one new mode, which is computed using a fixed-point algorithm, for example. The convergence of the method is illustrated in Fig. 2 for three different test cases, with respectively 8, 27 (as in Fig. 1), and 64 parameters, using a normalized residual as an error indicator:

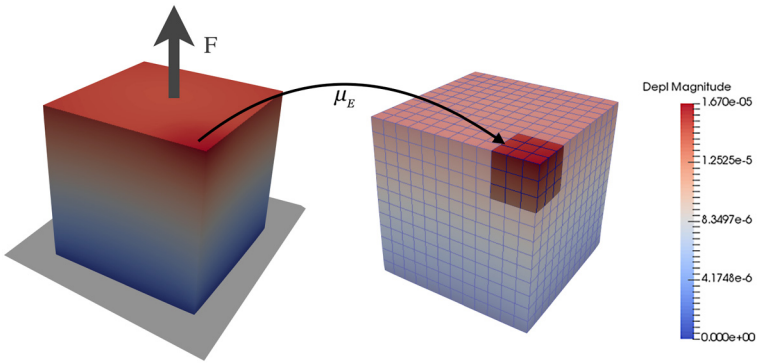

Fig. 1. Model problem with 27 parameters: particular solution and highlighting of a subdomain.

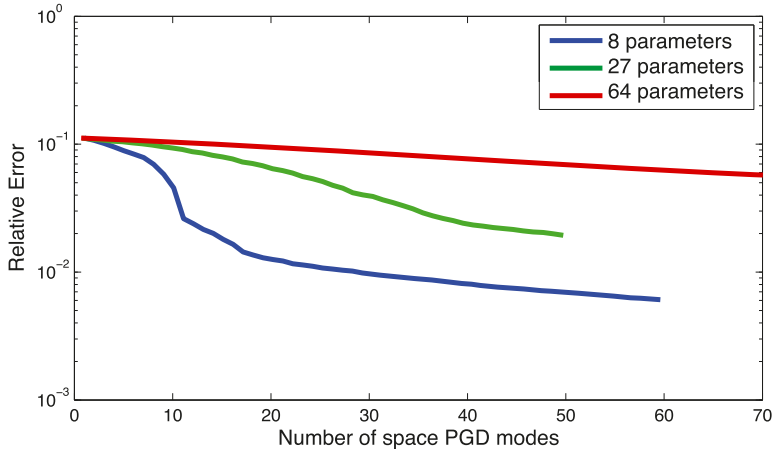

Fig. 2. Convergence curve of the classical PGD for three problems with different numbers of parameters.

$$\mathcal{E}^M = \frac{|||\boldsymbol{A}\underline{X}^M - \underline{F}_d|||}{|||\underline{F}_d|||} \qquad \text{with} \qquad |||\bullet|||^2 = \int_{\boldsymbol{\Sigma}_\mu} \bullet^T \boldsymbol{A}^{0^{-1}} \bullet \, \mathrm{d}\underline{\mu}$$

where $\boldsymbol{A}^0$ is the value of the operator $\boldsymbol{A}$ associated with the average value of the parameters. Such an indicator will describe only the quality of the PGD. Other sources of error such as the FE approximation will not be taken into account.

Convergence cannot be obtained in a reasonable number of iterations when the number of parameters is more than 30, and a new approach must be introduced.

4. The parameter-multiscale PGD – physical analysis

First, we analyze the impact of the parameters on the solution. Let us recall the parametric problem to be solved:

$$\boldsymbol{A}(\underline{\mu})\underline{X}(\underline{\mu}) = \underline{F}_d$$

Let us introduce $\boldsymbol{A}^0 = \boldsymbol{A}(\underline{\mu}_{\text{av}})$, the operator associated with the average value of the parameters (with the chosen definition of $\underline{\mu}$, we have: $\underline{\mu}_{\text{av}} = \underline{0} = \{0, 0, 0, \dots\}$), and let us suppose, for the sake of simplicity, that $\underline{F}_d$ does not depend on $\underline{\mu}$. One has:

$$\boldsymbol{A} = \boldsymbol{A}^0[\,\mathbf{1} - \underbrace{(\mathbf{1} - \boldsymbol{A}^{0^{-1}}\boldsymbol{A})}_{\boldsymbol{\Delta}}\,]$$

We set $\underline{X}_0 = \boldsymbol{A}^{0^{-1}}\underline{F}_d$. Using Neumann series, the solution can be written as:

$$\underline{X}(\underline{\mu}) \approx \underline{X}_0 + \underbrace{\Delta\underline{X}_0}_{\underline{X}_1(\underline{\mu})} + \underbrace{\Delta^2\underline{X}_0}_{\underline{X}_2(\underline{\mu})} + \cdots \tag{3}$$

where $\underline{X}_1$ is linear with respect to $\underline{\mu}$, and $\underline{X}_2$ quadratic with respect to $\underline{\mu}$. For most of the industrial applications, only a few terms of the development (3) will give a good approximation and then, the "curse of dimensionality" disappears. This is a consequence of the physical origin of the operator $\boldsymbol{A}$, which acts as a link between parameters. Let us explain this property in details.

On each subdomain Ω_E, we can separate the constant and parametric dependency on μ_E and suppose without loss of generality that $\boldsymbol{A}_E$ depends linearly on μ_E, which can be written as:

$$\boldsymbol{A}_E = \boldsymbol{A}_E^0 + \mu_E \overline{\boldsymbol{A}}_E$$

and then

$$\boldsymbol{A} = \bigwedge_{E\in\mathbf{E}} \boldsymbol{A}_E$$

where $\bigwedge_{E\in\mathbf{E}}$ corresponds to the assembly operation in the finite element context. We introduce the mask operator $\mathbf{I}_E$, allowing us to compute the global spatial extension $\underline{V}$ of the local field $\underline{V}_E$ through the relation $\underline{V} = \mathbf{I}_E \underline{V}_E$, which is equal to zero everywhere except on Ω_E. One can write: $\boldsymbol{A} = \bigwedge_{E\in\mathbf{E}} \boldsymbol{A}_E = \sum_{E\in\mathbf{E}} \mathbf{I}_E \boldsymbol{A}_E \mathbf{I}_E^T$. It follows:

$$\underline{X}_1(\underline{\mu}) = -\boldsymbol{A}^{0^{-1}} \left[\sum_{E\in\mathbf{E}} \mu_E \mathbf{I}_E \overline{\boldsymbol{A}}_E \mathbf{I}_E^T \underline{X}_0 \right] = \sum_{E\in\mathbf{E}} -\mu_E \boldsymbol{A}^{0^{-1}} \mathbf{I}_E \underbrace{\left[\overline{\boldsymbol{A}}_E \underline{X}_{0,E}\right]}_{\underline{Z}_E}$$

The term $\mathbf{I}_E \underline{Z}_E$ is associated with a self-equilibrated stress over Ω_E. Therefore, from Saint-Venant's Principle, the solution is localized in the neighborhood of the subdomain Ω_E, essentially over the subdomains sharing a common point with Ω_E denoted as $\mathbf{C}_E$. Let us set:

$$\underline{Z}_{1,E} = \boldsymbol{A}^{0^{-1}} \mathbf{I}_E \underline{Z}_E$$

which can be seen as negligible over the complement of $\mathbf{C}_E$. Let us define $\underline{Z}_{1,E}|_{\mathbf{C}_E}$, the restriction of $\underline{Z}_{1,E}$ over $\mathbf{C}_E$, we have:

$$\underline{Z}_{1,E} \simeq \mathbf{I}_{\mathbf{C}_E} \underline{Z}_{1,E}|_{\mathbf{C}_E}$$

and $\underline{X}_1(\underline{\mu}) = -\sum_{E\in\mathbf{E}} \mu_E \underline{Z}_{1,E}$; $\underline{X}_1$ is then linear with respect to $\underline{\mu}$ and $\underline{Z}_{1,E}$ is localized over the neighborhood $\mathbf{C}_E$ of Ω_E. A similar property, developed in [13], holds for $\underline{X}_2$:

$$\underline{X}_2(\underline{\mu}) \simeq \sum_{E\in\mathbf{E}} \mu_E^2 \underline{Z}_{2,E} + \sum_{E\in\mathbf{E}} \sum_{\substack{E'\in\mathbf{C}_E \\ E'\neq E}} \mu_E \mu_{E'} \underline{Z}_{2,EE'}$$

It follows from the Saint-Venant principle that the quadratic term of $\underline{X}_2(\underline{\mu})$ is such that $\underline{Z}_{2,E}$ is in practice localized over $\mathbf{C}_E$. The second term is linear with respect to each parameter.

The parameter-multiscale PGD that we propose is based on these properties. Thus we introduce two scales, "micro" and "macro", to describe the parameter space $\boldsymbol{\Sigma}_\mu$. The new representation that is proposed is:

$$\underline{X}_E(\underline{\mu}) = \sum_{i=1}^{N} \widetilde{\underline{X}}_E^{(i)} \prod_{E''\notin\overline{\mathbf{C}}_E} f_{E''}^{M(i)}(\mu_{E''}) \prod_{E'\in\overline{\mathbf{C}}_E} g_{EE'}^{m(i)}(\mu_{E'}) \tag{4}$$

where f^M and g^m are respectively "macro" and "micro" functions. It is essential to note that this description is given independently on each subdomain Ω_E. $\overline{\mathbf{C}}_E$ denotes a chosen neighborhood of Ω_E defining the "micro" impact in space of the parameter μ_E. For example, one can take the elements having a common point with Ω_E (i.e. $\overline{\mathbf{C}}_E = \mathbf{C}_E$), but other solutions have been tested in Section 6. Here, we will choose a linear discretization of the "macro" functions $f_{E''}^M$, and thus consider only their value on two points, $\mu_{E''} = \{\pm 1/2\}$.

The main difficulty of such a representation is the discontinuity of $\underline{X}(\underline{\mu})$ from one subdomain to another. To handle discontinuous displacements, the solver we have proposed is the so-called Weak-Trefftz Discontinuous Galerkin method (WTDG) introduced in [15] and extended to quasi-static loadings in [12] for the spatial discretization of our problem.

5. The parameter-multiscale PGD – computation

We are looking for the solution to (1), applied to the model problem of Section 2. The chosen parameters μ_E are associated with the stiffness of the material on the subdomain Ω_E. As an example, we can suppose that the stiffness matrix $\boldsymbol{K}_E$ coming from the Hooke law depends linearly on μ_E, and thus can be described by two variables ϵ and $\boldsymbol{K}_E^0$:

$$\boldsymbol{K}_E = \boldsymbol{K}_E^0 (1 + \epsilon \mu_E) \tag{5}$$

Initialization: The "average" problem is solved for the average value $\underline{\mu}_{\text{av}}$ of the parameters:

$$\boldsymbol{A}(\underline{\mu}_{\text{av}})\underline{X}_0 = \underline{F}_d$$

On each subdomain Ω_E, a strain $\boldsymbol{\varepsilon}_E^0$ and a stress $\boldsymbol{\sigma}_E^0 = \boldsymbol{K}_E^0\boldsymbol{\varepsilon}_E^0$ are defined. The local residual associated with the constitutive relation is:

$$\boldsymbol{R}_E^0 = \boldsymbol{\sigma}_E^0 - \boldsymbol{K}_E\boldsymbol{\varepsilon}_E^0$$

The local energetic norm of this residual, integrated over the parametric space, is normalized by the average deformation energy and will be used as an error indicator:

$$\mathcal{N}_E^2(\boldsymbol{R}_E^0) = \frac{\int_{\boldsymbol{\Sigma}_\mu} \boldsymbol{R}_E^0 {\boldsymbol{K}_E^0}^{-1} \boldsymbol{R}_E^0 \,\mathrm{d}\underline{\mu}}{\boldsymbol{\sigma}_E^0 {\boldsymbol{K}_E^0}^{-1} \boldsymbol{\sigma}_E^0}$$

Iteration $n+1$**:** After n iterations, the current approximated solution will be denoted by $\underline{X}^n$, and the residual will be of the form:

$$\boldsymbol{R}_E^n = \sum_{r=1}^{N_R} f_E^{(r)}(\underline{\mu})\boldsymbol{\sigma}_{R_E}^{(r)}$$

This residual could be compensated on the subdomain by:

$$\widetilde{\boldsymbol{\varepsilon}}_E^{n+1} = \boldsymbol{K}_E^{-1}\boldsymbol{R}_E^n \tag{6}$$

However, if we impose this strain brutally on the element Ω_E, the resulting stress field will not be equilibrated at the interface. Thus, we construct the operator $\boldsymbol{H}_E$ such as:

$$\overline{\boldsymbol{\sigma}}_E = \boldsymbol{H}_E\overline{\boldsymbol{\varepsilon}}_E$$

where the stress $\overline{\boldsymbol{\sigma}}_E$ comes from the reaction of all the domain when any strain $\overline{\boldsymbol{\varepsilon}}_E$ is imposed on Ω_E. Now, the residual will be perfectly compensated over the element Ω_E by $\boldsymbol{\varepsilon}_E^{n+1}$ if:

$$\boldsymbol{H}_E\boldsymbol{\varepsilon}_E^{n+1} = \boldsymbol{K}_E\boldsymbol{\varepsilon}_E^{n+1} - \boldsymbol{R}_E^n$$

The influence of $\boldsymbol{H}_E$ is very small compared to $\boldsymbol{K}_E$ and the strain field given by (6) gives very acceptable results. By adding locally the correction $\boldsymbol{\varepsilon}_E^{n+1}$ to the solution, the strain on the subdomain Ω_E will be exact. However, this local strain will also have a global influence $\underline{X}_{\boldsymbol{\varepsilon}_E}$, which can be determined by solving problem (7):

$$\begin{cases} \boldsymbol{A}(\underline{\mu})\left[\underline{X}_{\boldsymbol{\varepsilon}_E^{n+1}} - \underline{X}^n\right] = \underline{F} \\ \mathbf{I}_{\boldsymbol{\varepsilon}_E}\underline{X}_{\boldsymbol{\varepsilon}_E^{n+1}} = \boldsymbol{\varepsilon}_E^{n+1} \end{cases} \tag{7}$$

which is as difficult to solve as the initial problem (1) due to the parametric dependency of $\boldsymbol{A}$. Thus, we will simply compute the spatial influence of $\boldsymbol{\varepsilon}_E^{n+1}$ through the average operator. For each component $\boldsymbol{\varepsilon}_E^{(r)}$, $r \in \{1, \ldots, N_R\}$ of $\boldsymbol{\varepsilon}_E^{n+1}$, we note $f_E^{\prime(r)}$ the parametric dependency of the component. The simplified problem (8) is solved, with no parametric dependency:

$$\forall r \in \{1, \ldots, N_R\} \begin{cases} \boldsymbol{A}_0\left[\underline{\widetilde{X}}_{\boldsymbol{\varepsilon}_{R_E}}^{(r)} - \underline{X}^n\right] = \underline{F}_0 \\ \mathbf{I}_{\boldsymbol{\varepsilon}_E}\underline{\widetilde{X}}_{\boldsymbol{\varepsilon}_{R_E}}^{(r)} = \boldsymbol{\varepsilon}_{R_E}^{(r)} \end{cases} \tag{8}$$

Then, the solution can be globally updated:

$$\underline{X}^{n+1} = \underline{X}^n + \sum_{r=1}^{N_R} f_E^{\prime(r)}(\underline{\mu})\underline{\widetilde{X}}_{\boldsymbol{\varepsilon}_{R_E}}^{(r)}$$

To compute a complete iteration, this process is applied to every subdomain Ω_E of the space. This new correction will introduce a new residual on each element $E' \neq E$:

$$\boldsymbol{R}_{E'}^{n+1} = \boldsymbol{R}_{E'}^n + \sum_{r=1}^{N_R} f_E^{\prime(r)}(\underline{\mu})(\boldsymbol{K}^0 - \boldsymbol{K}_E)\underline{\widetilde{X}}_{\boldsymbol{\epsilon}_{R_E}|\boldsymbol{\epsilon}_{E'}}^{(r)}$$

This residual is then developed as a sum of PGD modes of $\overline{\boldsymbol{C}}_E$-type respecting the formulation (4).

Table 3
Convergence of the first two steps of the algorithm.

	Residual of the average solution	Residual after the first iteration	Residual after the second iteration
From 125 to 1000 parameters	29%	3.5–3.7%	0.49–0.55%

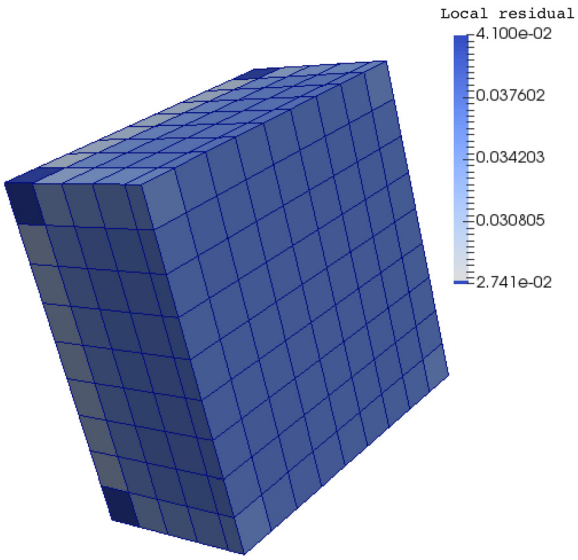

Fig. 4. Local residual after one complete iteration, cross-section of the cube (1000 parameters).

Table 5
Neighborhood influence: 125 parameters.

	Residual of the average solution	Residual after the first iteration	Residual after the second iteration
Chosen representation: micro function on neighboring elements	29%	3.6%	0.78%
Large number of micro functions (2 layers of neighbors)	29%	3.5%	0.49%
$\mathbf{C}_E = E$, micro function only on element Ω_E	29%	4.2%	0.82%

6. First results

The procedure of Section 5 has been applied to the model problem (1) with a stiffness variation of 50% around its average value, which is equivalent to choose $\epsilon = 1$ in Eq. (5). In the following problem, each subdomain is associated with a single element of the spatial decomposition, but the size of each subdomain could be increased without slowing the convergence of the algorithm. The space is meshed using cubic elements and the WTDG method has been applied to discretize the spatial fields, using a linear interpolation (WP1 elements).

After initialization, the residual associated with the average solution is equal to 29%, which can be analytically verified. Then two full iterations have been computed for a group of problems of different sizes, going from 125 subdomains to 1000. For each test case, the method gives sensibly identical global residuals for every number of parameters, as represented in Table 3.

As shown in [13], in one dimension, this method is strictly independent of the number of parameters. Fig. 4 shows that the repartition of the residuals is quasi-uniform.

Neighboring elements and macro–micro description

The choice of the number of neighboring elements is crucial in term of accuracy. In Fig. 6, we can see that the influence of each element is really localized in its neighborhood, as predicted by the Saint-Venant Principle. Several sizes of neighborhoods have been tested, and it appears that the micro description can be limited to one layer of elements without loosing too much accuracy. The first "layer" of elements $\mathbf{C}_E$ is here composed of all the elements sharing a full face with Ω_E and Ω_E itself, the second layer of all the elements sharing a face with $\mathbf{C}_E$, and so on.

Table 5 shows the order of magnitude of the influence of $\mathbf{C}_E$. Even with only one layer of neighboring elements, the accuracy keeps the same order of magnitude, which means in this 3D case that no more than seven micro functions are required per mode on each element. The representation (4) is well suited to this problem. We can even go further by

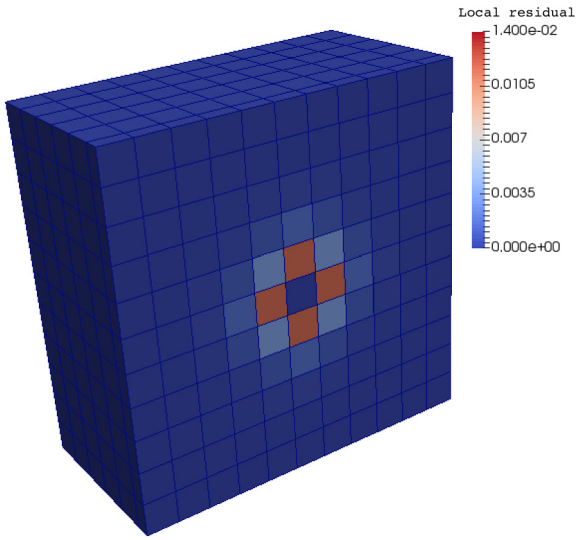

Fig. 6. Residual associated with the solution to the global problem (8) for a central element.

Table 7
125 parameters: norm of the residual for different levels of parametric variation.

Parametric variation	Residual of the average solution	Residual after the first iteration	Residual after the second iteration
10%	5.8%	0.08%	1.5e-3%
50%	29%	3.4%	0.43%
80%	46%	10%	3.8%
95%	55%	23%	14.5%

neglecting completely the influence of the parameter outside the first two layers, and save a lot of computational time with no noticeable loss of accuracy.

Influence of the parametric variations

By changing ϵ in formulation (5), we can change the variation range of the stiffness. As we can see in Table 7, this has an important influence on the convergence of the algorithm. For comparatively small variation (10%), the problem is much easier to solve than for a 50% variation, and the first iteration would provide a satisfactory solution. On the contrary, for very large parametric variations, a reduced model of the solution cannot be built easily. Indeed, the problem becomes very difficult to approximate, as it has to take into account fields that are very far from the average solution. For example, in a homogeneous cube (μ constant), a stiffness variation of 95% (i.e. $\varepsilon = 1.9$) gives a strain field associated with the minimum stiffness ($\underline{\mu} = -\underline{0.5}$) $\overline{20}$ times bigger than its average value. This value can be interpreted as a damage value of 0.95 over the whole material. Our algorithm cannot approximate such a solution, which is really hard to build as a sum of local variations, but the solution for a variation range of 80%, corresponding to a maximum damage value of 0.75, can still be approximated with a precision of about 4%. It is important to notice that, to reach this level of precision, the discretization level of the micro function must be high enough. For example, to get the results of Table 7, 100 points are used for each micro function. With only 20 points, the hardest cases such as the 95% one would not be corrected after the first iteration.

7. Conclusion

The proposed procedure provides an efficient way to compute an approximated solution for mechanical problems with a high number of local parameters. This procedure is very general and overcome one major limitation of the classical greedy procedures such as the standard PGD: no optimization problem has to be solved on the whole parametric domain. However, a large storage space is needed, as on each subdomain a full set of modes is locally defined in the parameter-multiscale PGD. The method can be easily extended to more global parameters. This can be done by considering that any parameter, local or global, can be discretized spatially on local subdomains.

The parameter-multiscale PGD seems to be a very promising reduced-order modeling technique for problems involving a large number of parameters. Further work will be devoted to the derivation of verification tools and to the extension to nonlinear problems such as viscoplastic ones. To take into account parameter values involving 0-rigidity elements is also a challenging question.

References

[1] F. Chinesta, P. Ladevèze (Eds.), Separated Representations and PGD-Based Model Reduction: Fundamentals and Applications, vol. CISM 554, Springer, 2014.
[2] P. Ladevèze, On algorithm family in structural mechanics, C. R. Acad. Sci. Paris, Ser. IIb 300 (2) (1985) 41–44.
[3] P. Ladevèze, The large time increment method for the analyse of structures with nonlinear constitutive relation described by internal variables, C. R. Acad. Sci. Paris, Ser. IIb 309 (2) (1989) 1095–1099 (in French).
[4] P. Ladevèze, On reduced models in nonlinear solid mechanics, Eur. J. Mech. A, Solids 60 (2016) 227–237.
[5] P. Ladevèze, Nonlinear Computational Structural Mechanics: New Approaches and Non-incremental Methods of Calculation, Springer-Verlag, New York, 1999.
[6] P. Ladevèze, New Methods with Conditioner for PGD Reduced Order Models, Technical report, LMT Cachan, France, 2014 (in French).
[7] A. Falco, W. Hackbusch, A. Nouy, Geometric Structures in Tensor Representations, work document, 2015, pp. 1–50.
[8] W. Hackbusch, Tensor Spaces and Numerical Tensor Calculus, Springer, 2012, series in ed.
[9] M. Billaud-Friess, A. Nouy, O. Zahm, A tensor approximation method based on ideal minimal residual formulations for the solution of high-dimensional problems, ESAIM: Math. Model. Numer. Anal. 48 (6) (2014) 1777–1806.
[10] S. Holtz, T. Rohwedder, R. Schneider, On manifolds of tensors of fixed TT-rank, Numer. Math. 120 (4) (2012) 701–731.
[11] I.V. Oseledets, Tensor-train decomposition, SIAM J. Sci. Comput. 33 (5) (2011) 2295–2317.
[12] P. Ladevèze, A New Method for the ROM Computation: The Parameter-Multiscale PGD, Technical report, LMT Cachan, 2016 (in French).
[13] P. Ladevèze, C. Paillet, D. Néron, Extended-PGD model reduction for nonlinear solid mechanics problems involving many parameters, Comput. Methods Appl. Sci. 46 (2018) 201–220.
[14] P. Ladevèze, J.-C. Passieux, D. Néron, The LATIN multiscale computational method and the proper generalized decomposition, Comput. Methods Appl. Mech. Eng. 199 (2010) 1287–1296.
[15] P. Ladevèze, New Variational Formulations for Discontinuous Approximations, Technical report, LMT Cachan, 2011 (in French).
[16] P. Ladevèze, H. Riou, On Trefftz and weak Trefftz discontinuous Galerkin approaches for medium-frequency acoustics, Comput. Methods Appl. Mech. Eng. 278 (2014) 729–743.
[17] A. Ammar, B. Mokdad, F. Chinesta, R. Keunings, A new family of solvers for some classes of multidimensional partial differential equations encountered in kinetic theory modelling of complex fluids. Part II: Transient simulation using space-time separated representations, J. Non-Newton. Fluid Mech. 144 (2–3) (2007) 98–121.